SUPPORTING INFORMATION

A multifunctional organogel for constructing artificial light harvesting systems with excellent energy transfer efficiency

Xinxian Ma,[#]* Jiahong Tang,[#] Tianqi Ren, Jiali Zhang, Yuehua Liang, Jiuzhi Wei, Enke Feng

College of Chemistry and Chemical Engineering, Ningxia Normal University, Guyuan 756000, People's Republic of China. Fax: 86 954 2079637; Tel: 86 954 2079637; E-mail: maxinxian@163.com

1. Experimental section

1.1 Materials

Polyvinyl alcohol (PVA, polymerization degree 1799, 98-99% alcoholysis), telmisartan (Tmt), ethylene glycol and dimethyl sulfoxide (DMSO) were provided by Shanghai Energy Chemical Co..

1.2 Preparation of organogel

The fluorescent organogel was prepared by esterification which just need a simple one-step reaction. The Tmt powder (0.2 g) was dissolved in DMSO (10 mL) and stirred for 30 minute at 120 ℃. Next, PVA (1.5 g) was added into the Tmt solution above, and reacted at 120 ℃ for 5h. After cooled to 50 ℃, added 1 mL glycol to the mixture and stirred well. Finally, poured the mixture into the surface dish, and it can be slowly formed into gel state for a while at -20 ℃.

1.3 Construction of ALHSs

The Tmt powder was dissolved in DMSO and stirred for 30 minute at 120 ℃. Next, PVA was added into the Tmt solution above, and reacted at 120 ℃ for 5h. After cooled the PVA/Tmt systems to 50 ℃, and added the fluorescent dyes glycol solution (different concentrations) to stirred continuously. The ALHSs based on organogels were completed.

2. Preparation method of xerogel

The obtained gel sample was soaked in anhydrous ethanol for a while and placed in a constant temperature oven at 70 ℃ for seven days, and the xerogel required for SEM   was   successfully   prepared.

Fig. S1. Frequency dependence of G' (storage modulus) and G" (loss modulus) for PVA/Tmt organogel at different Shear stress. Condition: 68 rad s^{-1} frequency, 10Hz constant frequency.

Fig. S2. Frequency dependence of G' (storage modulus) and G" (loss modulus) for PVA/Tmt/AYG organogel at different Shear stress. Condition: 68 rad s^{-1} frequency, 10Hz constant frequency.

Fig. S3. Frequency dependence of G' (storage modulus) and G" (loss modulus) for PVA/Tmt/RhB organogel at different Shear stress. Condition: 68 rad s^{-1} frequency, 10Hz constant frequency.

Fig. S4. Photos of the recyclability of PVA/Tmt/RhB organogel.

Fig. S5. UV−vis spectrum of PVA and PVA/Tmt organogels.

Fig. S6. (a) Fluorescence lifetime of PVA/Tmt organogel ([Tmt] = 1.5×10^{-6} mol. Monitored at 375 nm upon excitation at 333 nm). (b) Fluorescence lifetime of PVA/Tmt/AYG organogel ([Tmt] = 1.5×10^{-6} mol, [AYG] = 1.5×10^{-8} mol. Monitored at 375 nm upon excitation at 333 nm).

Table S1. Fluorescence lifetimes of PVA/Tmt organogel, PVA/Tmt/AYG organogel ([Tmt] = 1.5×10^{-6} mol, [AYG] = 1.5×10^{-8} mol, respectively).

Sample	τ_1/ns	RW_1[%]	τ_2/ns	RW_2[%]	τ/ns	χ^2
PVA/Tmt organogel	0.93	46.32	4.30	53.68	2.74	1.172
PVA/Tmt/AYG organogel	0.91	68.35	1.85	31.65	1.21	1.267

Fig. S7. Fluorescence decay profiles of PVA/Tmt organogel (red line, [Tmt] = 1.5 × 10⁻⁶ mol. Monitored at 375 nm upon excitation at 333 nm) and PVA/Tmt/AYG organogel assembly (black line, [Tmt] = 1.5 × 10⁻⁶ mol, [AYG] = 1.5 × 10⁻⁸ mol, Monitored at 375 nm upon excitation at 333 nm).

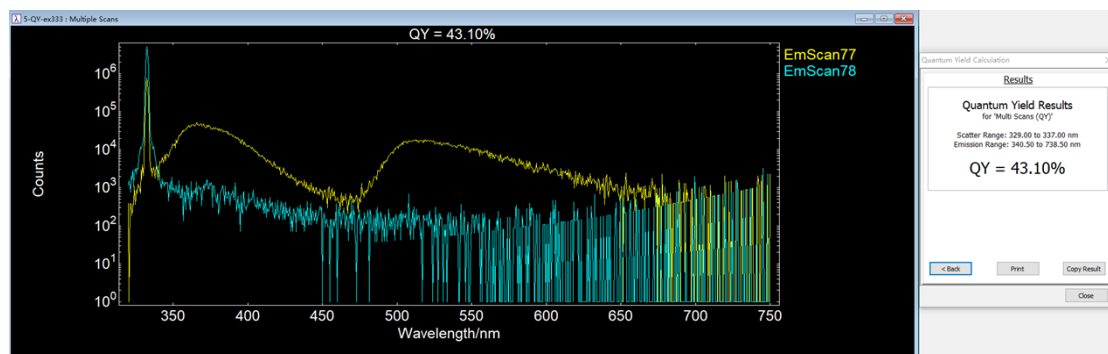**Fig. S8.** Quantum yield diagram of PVA/Tmt/AYG organogel with luminescence range of 450−700 nm ([Tmt] = 1.5 × 10⁻⁶ mol, [AYG] = 1.5 × 10⁻⁸ mol).

Fig. S9. (a) Fluorescence lifetime of PVA/Tmt organogel ([Tmt] = 1.5×10^{-6} mol. Monitored at 375 nm upon excitation at 350 nm). (b) Fluorescence lifetime of PVA/Tmt/RhB organogel ([Tmt] = 1.5×10^{-6} mol, [RhB] = 1.5×10^{-8} mol. Monitored at 375 nm upon excitation at 350 nm).

Table S2. Fluorescence lifetimes of PVA/Tmt organogel, PVA/Tmt/RhB organogel ([Tmt] = 1.5×10^{-6} mol, [RhB] = 1.5×10^{-8} mol, respectively).

Sample	τ_1/ns	RW_1[%]	τ_2/ns	RW_2[%]	τ/ns	χ^2
PVA/Tmt organogel	0.7645	74.42	2.73	25.58	1.27	1.278
PVA/Tmt/RhB organogel	0.7642	75.30	2.45	24.70	1.18	1.267

Fig. S10. Fluorescence decay profiles of PVA/Tmt organogel (red line, [Tmt] = 1.5 × 10^{-6} mol. Monitored at 375 nm upon excitation at 350 nm) and PVA/Tmt/RhB organogel assembly (black line, [Tmt] = 1.5 × 10^{-6} mol, [RhB] = 1.5 × 10^{-8} mol, Monitored at 375 nm upon excitation at 350 nm).

Fig. S11. Quantum yield diagram of PVA/Tmt/RhB organogel with luminescence range of 520−700 nm ([Tmt] = 1.5 × 10^{-6} mol, [RhB] = 1.5 × 10^{-8} mol).

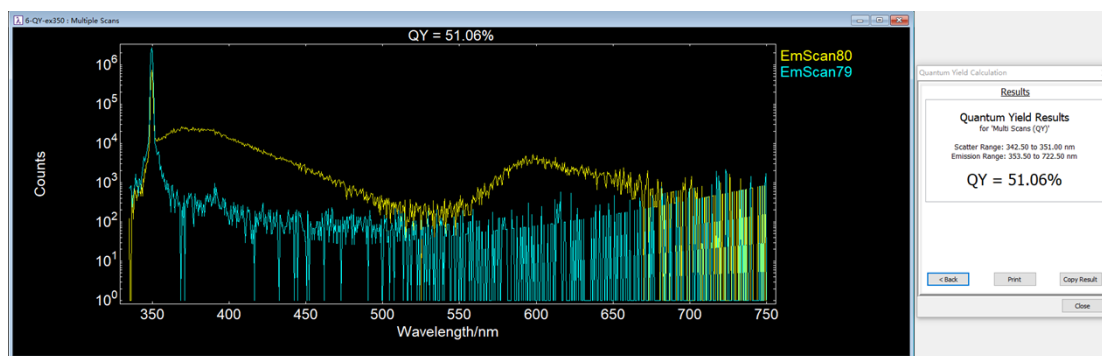**Fig. S12.** Fluorescence spectra of PVA/Tmt-AYG in the DMSO and ethylene glycol binary solven with different content of AYG (100:1, [Tmt] = 1.5×10^{-6} mol, [AYG] = 1.5×10^{-8} mol, and λ_{ex} = 333 nm).

Energy-transfer efficiency (Φ_{ET}) was calculated from spectra using equation S1.

$$\Phi_{ET} = 1 - I_{DA,333}/I_{D,333} \text{ (eq. S1)}^{1\text{-}3}$$

Where I_{DA} and I_{D} are the fluorescence intensities of the excitation of PVA/Tmt-AYG assembly (donor and acceptor) and Tmt assembly (donor), respectively at 333 nm.

The highest Φ_{ET} value was calculated as 82.77% in solvent, measured under the condition of [Tmt] = 1.5×10^{-6} mol, [AYG] = 1.5×10^{-8} mol, and λ_{ex} = 333 nm.

Fig. S13. Fluorescence spectra of PVA/Tmt-RhB in the DMSO and ethylene glycol binary solven with different content of RhB (100:1, [Tmt] = 1.5×10^{-6} mol, [RhB] = 1.5×10^{-8} mol, and λ_{ex} = 350 nm).

Φ_{ET} was calculated from spectra using equation S2.

$$\Phi_{ET} = 1 - I_{DA,350}/I_{D,350} \text{ (eq. S2)}^{[1\text{-}3]}$$

Where I_{DA} and I_D are the fluorescence intensities of the excitation of PVA/Tmt-RhB assembly (donor and acceptor) and Tmt assembly (donor), respectively at 411 nm.

The highest Φ_{ET} value was calculated as 16.58% in solvent, measured under the condition of [Tmt] = 1.5×10^{-6} mol, [RhB] = 1.5×10^{-8} mol, and λ_{ex} = 350 nm.

Fig. S14. Line chart of energy transfer efficiency of PVA/Tmt/AYG and PVA/Tmt/RhB organogel at different proportions.

Fig. S15. Red line: Fluorescence spectra of PVA/Tmt-AYG in the DMSO and ethylene glycol binary solven, which was normalized according to the fluorescence intensity at 365 nm of the black line (λ_{ex} = 333 nm) ([Tmt] =1.5 × 10^{-6} mol, [AYG] = 1.5 × 10^{-8} mol); the black line represents the fluorescence spectrum of PVA/Tmt.

The antenna effect (AE) was calculated based on the excitation spectra using equation S3.

$$AE = (I_{DA,333} - I_{D,333})/I_{A,333} \text{ (eq. S3)}$$

Where $I_{DA,333}$ and $I_{DA,333}$ are the fluorescence intensities at 500 nm with the excitation of the donor at 333 nm and the direct excitation of the acceptor at 333 nm, respectively. $I_{D,333}$ is the fluorescence intensities at 500 nm of the PVA/Tmt assembly, which was normalized with the PVA/Tmt-AYG assembly at 376 nm.

The antenna effect value was calculated as 16.8690 in the DMSO and ethylene glycol binary solven, measured under the condition of [Tmt] = 1.5 × 10^{-6} mol, [AYG] = 1.5 × 10^{-8} mol.

Fig. S16. Red line: Fluorescence spectra of PVA/Tmt-RhB in the DMSO and ethylene glycol binary solven, which was normalized according to the fluorescence intensity at 387 nm of the black line (λ_{ex} = 350 nm) ([Tmt] =1.5 × 10^{-6} mol, [RhB] = 1.5 × 10^{-8} mol); the black line represents the fluorescence spectrum of PVA/Tmt.

The antenna effect (AE) was calculated based on the excitation spectra using equation S4.

$$AE = (I_{DA,350} - I_{D,350})/I_{A,350} \text{ (eq. S4)}$$

Where $I_{DA,350}$ and $I_{DA,350}$ are the fluorescence intensities at 589 nm with the excitation of the donor at 350 nm and the direct excitation of the acceptor at 350 nm, respectively. $I_{D,333}$ is the fluorescence intensities at 589 nm of the PVA/Tmt assembly, which was normalized with the PVA/Tmt-RhB assembly at 387 nm.

The antenna effect value was calculated as 1.7889 in the DMSO and ethylene glycol binary solven, measured under the condition of [Tmt] = 1.5 × 10^{-6} mol, [RhB] = 1.5 × 10^{-8} mol.

References

(1) R. Gao and D. Yan, *Chem. Sci.*, 2017, **8**, 590−599.

(2) S. Guo, Y. Song, Y. He, X. Hu and L. Wang, *Angew. Chem. Int. Ed.*, 2018, **57**, 3163−3167.

(3) M. Hao, G. Sun, M. Zuo, Z. Xu, Y. Chen, X. Hu and L. Wang, *Angew. Chem. Int. Ed.*, 2020, **59**, 10095−10100.